Interpretation of Lamellar Electron Diffraction Data from Phospholipids

Douglas L. Dorset and Andrew K. Massalski

Electron Diffraction Department, Medical Foundation of Buffalo, Inc., 73 High Street, Buffalo, New York 14203

John R. Fryer

Chemistry Department, University of Glasgow, Glasgow G 12 8 QQ Scotland

Z. Naturforsch. **42 a**, 381–391 (1987); received October 8, 1986

Lamellar electron diffraction intensity data from a series of optically active 1,2-diradyl phosphatidylethanolamines were used to determine the probable crystal packing, based on translational fitting of the molecular conformation found in the x-ray crystal structure of a dilauroyl homolog. All crystal structures are shown to be similar to one another. A packing model similar to that found from the analysis of lamellar x-ray data from the dimyristoyl homolog is obtained when the measured electron diffraction data are corrected for the curvilinear lamellar deformations seen in direct low dose lattice images.

Crystal Structure Analysis, Crystal Distortion

Introduction

Two decades ago, considerable effort was devoted to the structure analysis of multilamellar biomembranes, such as myelin, using one-dimensional x-ray diffraction data from well oriented samples [1, 2], a process which often involved interesting techniques for determining crystallographic phases [1–5]. Concomitant work was also carried out on oriented multilayers of pure phospholipids, and also those incorporating cholesterol [6, 7]. The most unequivocal structure analysis of such systems was based on neutron diffraction data which followed the position of deuterium labels in the acyl chains and polar group [8–10], giving conformational results consistent with single crystal structure analyses on a small number of diacyl phospholipids [11–15].

After the first crystal structure was reported for a diacyl phosphatidylethanolamine [11], the resultant structural model was used to analyze lamellar x-ray data from a homolog [16], basing this determination on rigid body refinement of a presumed invariant structural conformation for which only overall thermal parameters and molecular shift were permitted to change. Using epitaxial crystallization techniques originally designed for the orientation of polymethylene chain polymers [17], thin lath-like microcrystals of various phospholipids were also grown [18] which give lamellar electron diffraction intensities similar in resolution to the best powder x-ray data from oriented bulk specimens. Although analyses of electron diffraction data based on the known phosphatidylethanolamine crystal structure result in crystallographic residuals similar to the earlier powder x-ray study [16], the refined structures were found to have different packing arrangements.

While it is true that phosphatidylethanolamines can crystallize as polymorphic forms [19, 20], available electron diffraction data such as the lamellar spacings [18, 21] indicate that the epitaxially crystallized material should be similar to the structural forms investigated by x-ray diffraction methods. This expectation is supported by the determination of methylene subcell packing with electron diffraction data from solution crystallized samples which also indicate that the molecular chains are untilted [20, 22]. A survey of the known phospholipid crystal structures indicates some conformational freedom in the headgroup region [23] but, by contrast, the conformation of the diacyl glycerol moiety is shown to be extremely conservative [23], with the same features shown for a variety of phospholipids [11–14], encompassing

Reprint requests to Dr. D. L. Dorset, Electron Diffraction Department, Medical Foundation of Buffalo, Inc., 73 Hight St., Buffalo, New York 14203, USA.

0340-4811 / 87 / 0400-0381 $ 01.30/0. – Please order a reprint rather than making your own copy.

optically active as well as racemic materials in addition to the numerous headgroup species and conformations. Specifically, the molecular packing and conformation of optically active phosphatidylethanolamines is shown by neutron diffraction analysis [10] to be very similar to the racemic compound [11, 12] even when an acetic acid solvent molecule is missing from the headgroup region. For this material this similarity includes the headgroup conformation as well as the axial displacement of acyl chains in the diglyceride portion.

Because the use of electron diffraction data for quantitative structure analyses is still in an early stage of development, it is important to find reasons for discrepancy noted in the earlier determination [19]. From a practical standpoint, since numerous data from direct lattice images and electron diffraction have been obtained from many epitaxially oriented phospholipid samples [24] not yet crystallized for single crystal x-ray studies, as well as their solid solutions (D. L. Dorset and A. Massalski, unpublished data), is also will be useful to compare future analyses to the results obtained from a system which is already well defined, such as the phosphatidylethanolamines.

Materials and Methods

Crystallization of Phospholipids

A homologous series of chiral 1,2-diacyl phosphatidylethanolamines (dilauroyl, dimyristoyl, dipalmityol) as well as one chiral 1,2-dialkyl phosphatidylethanolamine (dihexadecyl) were purchased from Calbiochem-Behring (San Diego, Ca.) and were used without further purification. Epitaxial crystallization on a naphthalene substrate was carried out according to the procedure of Wittmann et al. [17] as follows: A small amount of the lipid is dissolved in chloroform and a drop of this solution is allowed to evaporate to dryness on a freshly cleaved mica sheet. Carbon covered electron microscope grids are placed over this lipid-containing area and naphthalene crystals are then sprinkled over the surface. The other half of the mica sheet is placed over this physical mixture to form a sandwich and this is moved along a thermal gradient until the naphthalene melts and flows into the space between the sheets, meanwhile solvating the phospholipid layer. The specimen is then cooled so that the naphthalene crystallization at the eutectic can direct the epitaxial crystallization of the lipid. This places the longest crystallographic axis parallel to the best developed crystal face in contrast to crystallization from solution. The sheets are mechanically separated and the naphthalene removed by sublimation *in vacuo* to leave the epitaxial phospholipid crystals on the grid surface.

Electron Diffraction Data Collection and Microscopy

Selected area electron diffraction patterns at 100 kV were recorded on x-ray film (Kodak DEF-5) using a JEOL JEM-100 B electron microscope operated at low incident beam current density to minimize radiation exposure of the sample. Intensity data were obtained from the photographic films by integration under scans made on a Joyce Loebl MkIIIC flat bed microdensitometer.

Low dose electron micrographs of the thin crystals were obtained according to a method given by Fryer [25]. At nearly the same incident beam current as for electron diffraction, images at various values of objective lens defocus were recorded on the same x-ray film at an operating magnification of 20,000×. After a focal series was photographed, the integrity of the specimen was ascertained by observation of the electron diffraction patterns.

Calculations

Kinematical structure factors were calculated in the usual way, i.e.

$$F_{00l} = \sum_{l} f_j' \exp 2\pi i (\boldsymbol{r}_j \cdot \boldsymbol{s}_l),$$

where f_j' is the Doyle-Turner [26] scattering factor corrected for isotropic thermal motion, i.e.

$$f_j' = f_j \cdot \exp(-B \sin^2 \theta/\lambda^2),$$

$\boldsymbol{r}_j$ is the atom position in the unit cell and $\boldsymbol{s}_l$ is the reciprocal lattice vector. Translational shifts along c are calculated with a suitable computer program based on the function [27], $F_{00l} = 2(aA - bB)$, where $a = \cos 2\pi l z_a$, $b = \sin 2\pi l z_a$,

$$A = \sum_j f_j' \cos 2\pi l z_j \quad \text{and} \quad B = \sum_j f_j' \sin 2\pi l z_j,$$

for which z_a is the fractional coordinate of an arbitrary origin and z_j are atomic coordinates with respect to this origin.

One-dimensional Patterson functions were also calculated in the usual way, i.e.

$$P(w) = \sum_{l} |F_{00l}|^2 \cos 2\pi l z,$$

and electrostatic potential maps (electron diffraction analog to an electron density map) were computed in an analogous fashion to the x-ray case, i.e.

$$\varrho(z) = V_0 + 2 \sum_{1}^{l} F_{00l} \cos 2\pi l z,$$

where V_0 is the mean inner potential of the structure and the F_{00l} are suitably scaled, phased structure factors. It will be noted that centrosymmetry is assumed for this reciprocal lattice row based on previous structural analysis on phospholipids and biomembranes [1–5]. (This is the consequence of a 2_1-screw axis perpendicular to the longest unit cell axis as found in the known phospholipid crystal structures [11–15].)

N-beam dynamical corrections were made in either of two ways. In early hand calculations, a phase grating approximation [28] was used, i.e.

$$\Phi_{00l} = \mathcal{F} q(z) = \delta - i\sigma \Delta t F(00l) + \frac{\sigma^2 \Delta t^2}{2!} F(00l) * F(00l) + \ldots,$$

where the operation "$*$" denotes convolution. Later a full multislice calculation [28] was carried out using a computing package from the Arizona State University facility for high resolution electron microscopy. In the latter calculation the structural model was tilted 16° around [001] to allow only $00l$ reflections to contribute to the structure factor convolutions. Because only low angle data are used (hence a minor deviation of the Ewald sphere from the reflection center) the difference between the two calculations is very small.

Results

Overview

A representative electron diffraction pattern from an epitaxially crystallized phosphatidylethanolamine is shown in Figure 1. Lamellar spacings of the phospholipids used in this study are given in Table 1 in comparison with literature values. Details of the crystal texture are revealed in high resolution electron micrographs shown in Figure 2. As discussed elsewhere [24], the undulation of the lamellae expains the arcing of the $00l$ diffraction data.

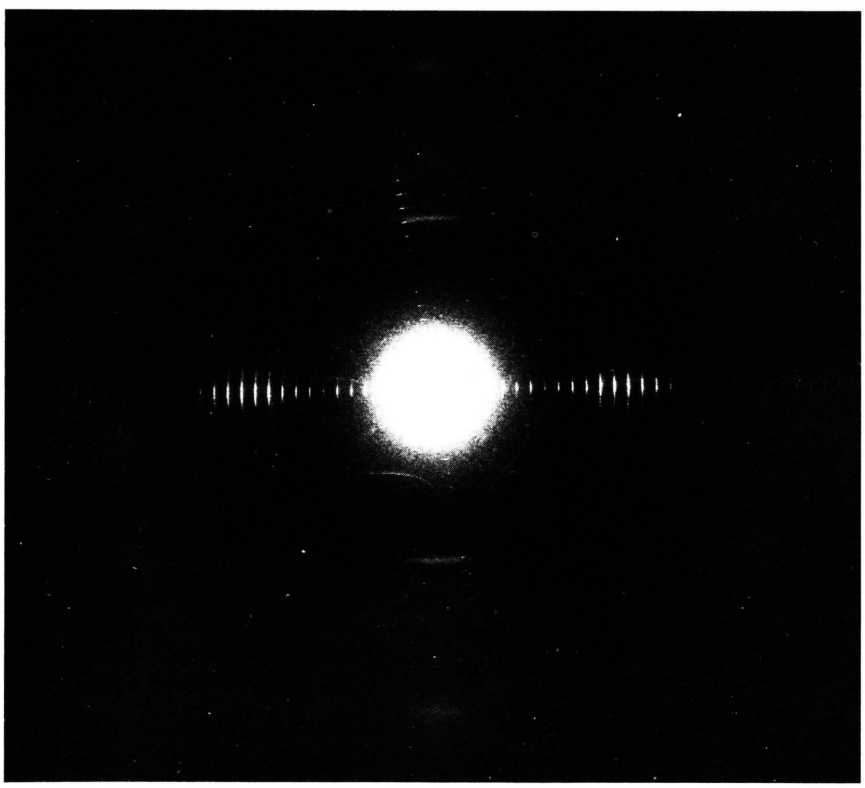

Fig. 1. Electron diffraction pattern of 1,2-dihexadecyl-*sn*-glycerophosphoethanolamine (DHPE) epitaxially crystallized on naphthalene. Note arcing of lamellar reflections.

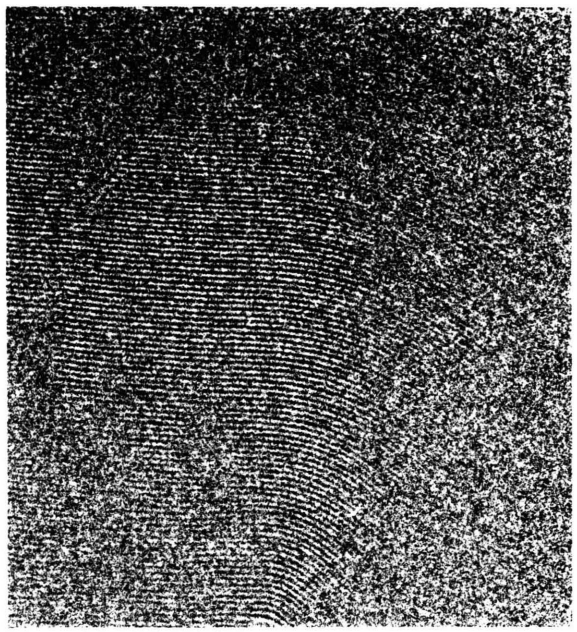

Fig. 2. Low dose lattice image of 1,2-dipalmitoyl-*sn*-glycerophosphoethanolamine epitaxially crystallized on naphthalene: Note the curvature of lamellae which accounts for the arcing of the electron diffraction patterns as in Figure 1 (see also [24]). Similar images have been obtained from other epitaxially-crystallized phosphatidylethanolamines examined in this study.

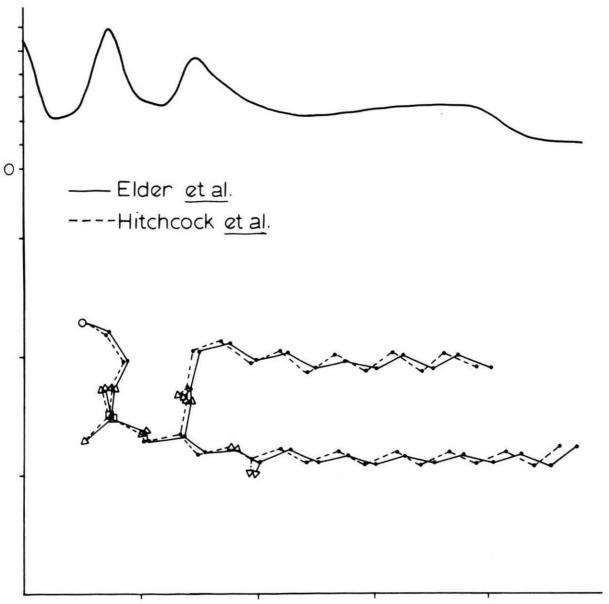

Fig. 3. Crystal structure of 1,2-dilauroyl-*rac*-glycerophosphoethanolamine as determined initially by Hitchcock et al. [11] and then refined by Elder et al. [12]. The view represents the asymmetric unit in the (001) projection of their crystal structure where the abscissa and ordinate are respectively parallel to their *a* and *b* axes. (In our study, we have relabeled their longest unit cell *a* axis as "*c*" to conform to usual convention in the crystallography of lipids.) Note that there are slight differences in atom positions. These structures were used as models for rigid body refinement after appropriate extension of the polymethylene chains (see text). A one-dimensional plot of electron density is shown above for this structure. (In this plot, the position of the acetic acid solvent molecule is shown near the origin although it is not represented in the molecular drawing.)

Table 1. Lamellar spacing of chiral diradyl phosphatidylethanolamines used for quantitative electron diffraction structure analysis.

Compound	d_{001}	
	This study	Literature
1,2-Dilauroyl-*sn*-glycerophosphoethanolamine (DLPE) diffraction resolution: $l = 14$	47.7 ± 0.5 Å	45.2 Å (rac) [42] 47.8 Å (rac) [16]
1,2-Dimyristoyl-*sn*-glycerophosphoethanolamine (DMPE) diffraction resolution: $l = 15$	49.2 ± 0.4 Å	50.0 Å (rac) [20] 49.9 Å (rac) [42] 49.5 Å (rac) [16]
1,2-Dipalmitoyl-*sn*-glycerophosphoethanolamine (DPPE) diffraction resolution: $l = 16$	55.7 ± 0.5 Å	55.0 Å (sn) [18] 55.2 Å (rac) [20] 55.3 Å (rac) [42]
1,2-Dihexadecyl-*sn*-glycerophosphoethanolamine (DHPE) diffraction resolution: $l = 16$	55.2 ± 0.5 Å	55.6 ± 0.5 Å (sn) [19]

Because of the somewhat coarse sampling interval used for translation of the model structure there are ambiguities in the reported one-dimensional x-ray structural analysis of 1,2-dimyristoyl *rac*-phosphoethanolamine based on the crystal structure of its dilauroyl homolog. This determination was repeated starting with slightly different structural models given in earliest [11] and later [12] reports of the dilauroyl structure (Fig. 3) and using the reported x-ray data [16]. To construct the dimyristoyl model, the chains were extended along their axes by the average translation value per methylene repeat (1.27 Å) and the position of the outermost methyl was placed at $z = 0.5000$ in the appropriate unit cell. The temperature factors were assigned according to the scheme given by Hitchcock et al. [16], hence

$$B(z) = (C + 4.0 + 108\,(z)^2)\ \text{Å}^2 \qquad (1)$$

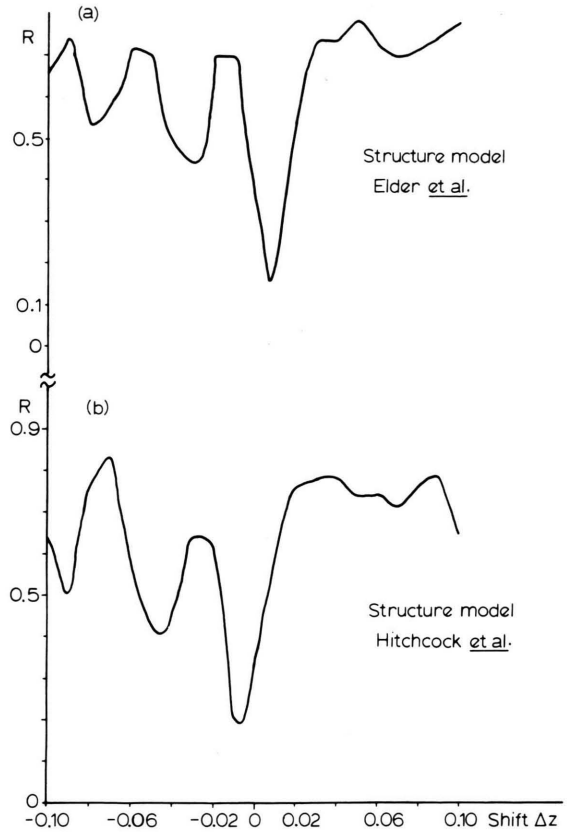

Fig. 4. Rigid body structural analysis with published lamellar x-ray data from 1,2-dimyristoyl-*rac*-glycero-phosphoethanolamine using models based on the two structures given in Figure 3. The occurrence of minima at slightly different shift positions merely indicate that the polar group positions of the respective models were at different *relative* locations because the initial z fractional coordinate of the outer methyl carbon is initially at $z = 0.5$. The sampled shift values in the translation search are at finer intervals than in the original analysis [16], revealing the presence of several minima rather than the single broad one depicted earlier.

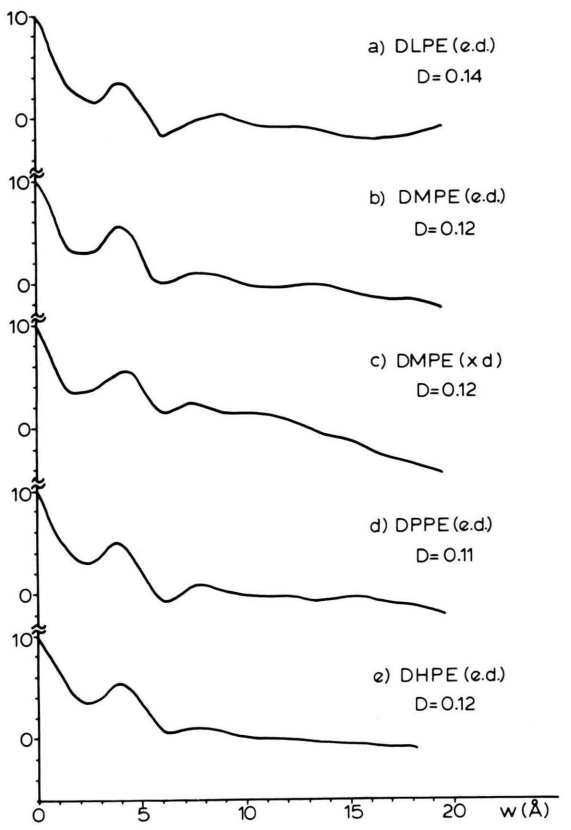

Fig. 5. One-dimensional Patterson syntheses for experimental electron and x-ray diffraction data considered in this work, demonstrating the basic identity of these data which indicate a large peak near 4.0 Å and a second between 7 and 8 Å. When the electron diffraction data are corrected for crystal texture (see text) the Patterson maps are still similar in appearance, although peaks corresponding to longer vectors are more discernable.

for all atoms except for phosphorus where

$$B(z) = (C + 3.0)\ \text{Å}^2. \qquad (2)$$

As in their study, $C = 25\ \text{Å}^2$. Results of rigid body search along z are shown in Fig. 4 for the two starting models. The results are basically the same, giving a minimum for the phosphorus position at 0.0515 (49.5 Å) = 2.55 Å for the model of Elder et al. [12] and at 0.0497 (49.5 Å) = 2.46 Å for the model of Hitchcock et al. [11]. It is apparent therefore that the headgroup position is the most important factor for this structure determination. Due to the presence of an acetic acid solvent molecule, the polar group packing of the multilayer cannot be directly compared to the homolog crystal structure but it is consistent with the phosphorus z-coordinate for a lysophosphatidylethanolamine [29] ($z \cdot c = 2.24$ Å). Observed and calculated structure factors are listed in Table 3.

Patterson Synthesis

Patterson functions are shown in Fig. 5 for the data sets considered in this study. The electron diffraction intensities were taken as they were obtained from integration of densitometer traces without further corrections and placed on a common scale. These are also compared to a Patterson synthesis on lamellar x-ray data from the study of DMPE by Hitchcock et al. [16]. An analysis of the

Table 2. Results of rigid body refinements on 1,2-dihexadecyl-*sn*-phosphoethanolamine based on electron diffraction intensities.

Model	Phosphorus position		
	Start	Finish	*R*-value
1. Perfect crystal low temperature factors	0.0379[a]	0.0079	0.26
		−0.0321	0.24
($C = 0.0$ Å^2)	0.0505[b]	0.0055	0.26
		−0.0345	0.28
2. Perfect crystal high temperature factors			
a) whole molecule	0.0505	0.0405*	0.35
($C = 25$ Å^2)		0.0005	0.33
b) alkyl chains	0.0505	0.0055	0.27
($B_c = 79$ Å^2)			
3. Distorted crystal low temperature factors			
a) "mosaic" correction	0.0505	0.0405*	0.30
for curvilinear	0.0379	0.0379*	0.35
lamellae			
b) Gaussian correction	0.0379	0.0079	0.28
$l > 8$			
c) Gaussian correction	0.0379	0.0379*	0.34
similar to mosaic model			

[a] This starting position corresponds to the most highly refined crystal structure of DLPE by Elder et al. [12].
[b] This starting position corresponds to the first structure reported for DLPE by Hitchcock et al. [11].
* Correct structure.

Table 3. Calculated and observed structure factor values for 1,2-diradyl glycerophosphoethanolamines.

rac DMPE (x-ray)			*sn* DHPE (e.d.)		
l	$\lvert F_0 \rvert$	F_{calc}	l	$\lvert F_0 \rvert$	F_{calc}
1	13.49	12.99	1	1.20	2.22
2	2.04	0.54	2	0.61	−0.26
3	2.50	0.26	3	1.24	1.20
4	5.26	−6.20	4	0.70	−0.82
5	1.05	−2.07	5	0.91	0.09
6	1.95	−2.07	6	0.54	−0.84
7	1.70	−1.23	7	0.72	−0.34
8	1.75	−2.73	8	0.20	−0.43
9	4.29	−4.16	9	0.62	−0.78
10	3.76	−3.48	10	0.96	−0.43
11	5.53	−5.58	11	1.04	−1.24
12	4.43	−3.96	12	1.65	−1.44
13	6.00	−6.37	13	1.61	−1.86
14	3.73	−5.09	14	1.60	−1.72
15	2.46	−3.20	15	1.47	−1.54
			16	1.19	−1.04
	$R = 0.19$			$R = 0.30$	

DMPE Patterson map was reported by Khare and Worthington [30]. Three peaks at 4, 7.2 and 11.2 Å (see Fig. 5) were interpreted on the basis of intermolecular vectors, respectively between the phosphoethanolamine groups (4 Å) and the polar portion of the diglyceride (11.2 Å), as well as an intermolecular cross vector between these regions (7.2 Å). This was used to justify a molecular conformation with the polar headgroup bent parallel to the bilayer surface as indicated in other studies [10].

Although some difference exists between the *relative* scattering factor values in electron diffraction when compared to x-ray diffraction, the computed Patterson functions for the electron diffraction data sets are again quite similar to the one given for the x-ray data set (Fig. 5), i.e. the major peak is at 4 Å with a second peak between 7 and 8 Å. The exact position of the third peak is less clear. The detectibility of phosphorus, defined

$$D = \sum f_p^2 / \sum f_{\text{light atom}}^2 ,$$

is approximately the same in electron and x-ray diffraction for the total phospholipid molecule as indicated in Figure 5. However the relative values of the nitrogen and oxygen scattering factors are less than that of carbon in electron diffraction while they are greater in x-ray diffraction. It is apparent, therefore, that phosphorus scattering will have a major role in the electron diffraction from these specimens, although the combined scattering from aligned lighter atoms can also play a similar role to the x-ray scattering case. Given the features of our experimental Patterson maps and the molecular alignment indicated from electron diffraction experiments on solution crystallized samples [19, 11], we carry out our translational search using the untilted molecular packing found for the *racemic* dilauroyl homolog [11, 12] also preserving the molecular conformation with the anticipation that a solution will be found with polar groups spaced across the polar boundary near $w = 4.0$ Å. In the ensuing discussion this distance will be assessed by finding the position of the phosphorus atom at the *R*-value minimum.

Rigid Body Translational Search of Electron Diffraction Data

Rigid body translational searches were carried out for the various data sets used to create the

Patterson maps in Fig. 5 after suitable chain length adjustment for the respective molecules in the appropriate unit cell length as discussed above. (For the ether-linked phospholipid, the carbonyl oxygens are excluded from in the structure factor calculations.) In these analyses, three types of models were considered, as discussed in the following and reviewed in Table 2 for the dihexadecyl compound, in an attempt to discover what factors might cause this solution technique to find a false minimum.

(a) Low Temperature Factors, Perfect Crystal

A rigid body model with temperature factors based on (1) and (2) were used with $C = 0.0$ Å^2 to simulate a crystal packing with temperature factors similar to the reported crystal structure of the dilauroyl homolog [11, 12]. Observed structure factor values were obtained simply as square roots of the observed intensity. A representative translational search is shown in Fig. 6 for the dihexadecyl compound, which is similar to results given earlier from values obtained with a hand calculator [19]. These data, as well as those from the dimyristoyl and dipalmitoyl materials, indicate that structural models at two minima give similarly low residuals. These minima correspond to phosphorus coordinates respectively in the ranges 0.30 to 0.44 Å and -1.61 to -1.92 Å, values which are clearly incompatible with the above analyses of x-ray data and the Patterson syntheses on all data sets. Dynamical calculations are found to lower the value of these residuals but do not change the positions of the minima.

(b) High Temperature Factors, Perfect Crystal

Two alternate models were attempted which imposed higher temperature factors on molecular moieties. Using the value $C = 25$ Å^2 in (1) and (2) for the dimyristoyl and dihexadecyl phosphatidylethanolamines, rigid body translation gives residual minima respectively in the translation intervals 2.23 to 2.33 Å and 0.03 to 0.60 Å for the phosphorus atom position. If the temperature factors for the molecular moiety in the polar region are adjusted to the values in (1) and (2) for $C = 0.0$ Å^2 but with $B = 70$ Å^2 for outer chain atoms, similar minima are found e.g. for the dipalmitoyl material. The *R*-factor minima however are not as low as found previously (Figure 6).

(c) Corrections for Crystal Texture

From the appearance of the electron diffraction pattern in Fig. 1 as well as the lattice images in Fig. 2, the crystals used in this structure analysis are far from being perfect. The curvilinear distortion of the lamellar stacking was shown by Vainshtein [31] be equivalent to a distortion of the second kind, commonly referred to as paracrystallinity. Although paracrystalline, the crystals are not mosaic in the usual sense (i.e. there is no pronounced subdivision of the crystals by defects into crystallites). The correction of experimental data for such a texture should nevertheless be similar to a mosaic correction, particularly if the densitometer scans do not record the total intensity of a reflection [32]. Following Vainshtein [33], the correction for the observed intensity I^{obs}_{00l} can be written as

$$|F_{00l}|_{\text{obs}} = (I^{\text{obs}}_{00l} \cdot d^*_{00l})^{1/2} \tag{3}$$

or, since d^*_{00l} is proportional to the Miller index l,

$$|F_{00l}|_{\text{obs}} \propto (I_{00l} \cdot l)^{1/2},$$

as is often used to correct lamellar diffraction data from biomembranes [1–5]. Such corrections of lamellar electron diffraction data for all phospholipids results in a single residual minimum after rigid body refinement (Fig. 6), giving a phosphorus position in the range 2.08 to 2.76 Å. The *R*-value minima are lower than the thermal model (b) given above but not quite as low as in the first perfect crystal model.

Another type of correction may be envisioned. If the error in intensity measurement is only due to the arced higher order reflection falling outside the width of the densitometer scan, then for a Gaussian function

$$f(x) = \exp(-h^2 x^2/l^2)$$

the half width l/h of a reflection along $x \perp z^*$ is dependent on the Miller index l. If reflections beyond say $l = 8$ are incompletely measured by the densitometer, the observed intensity can be corrected after finding the fraction of the Gaussian area outside the scan width. After numerical integration of such a Gaussian model and a translational search

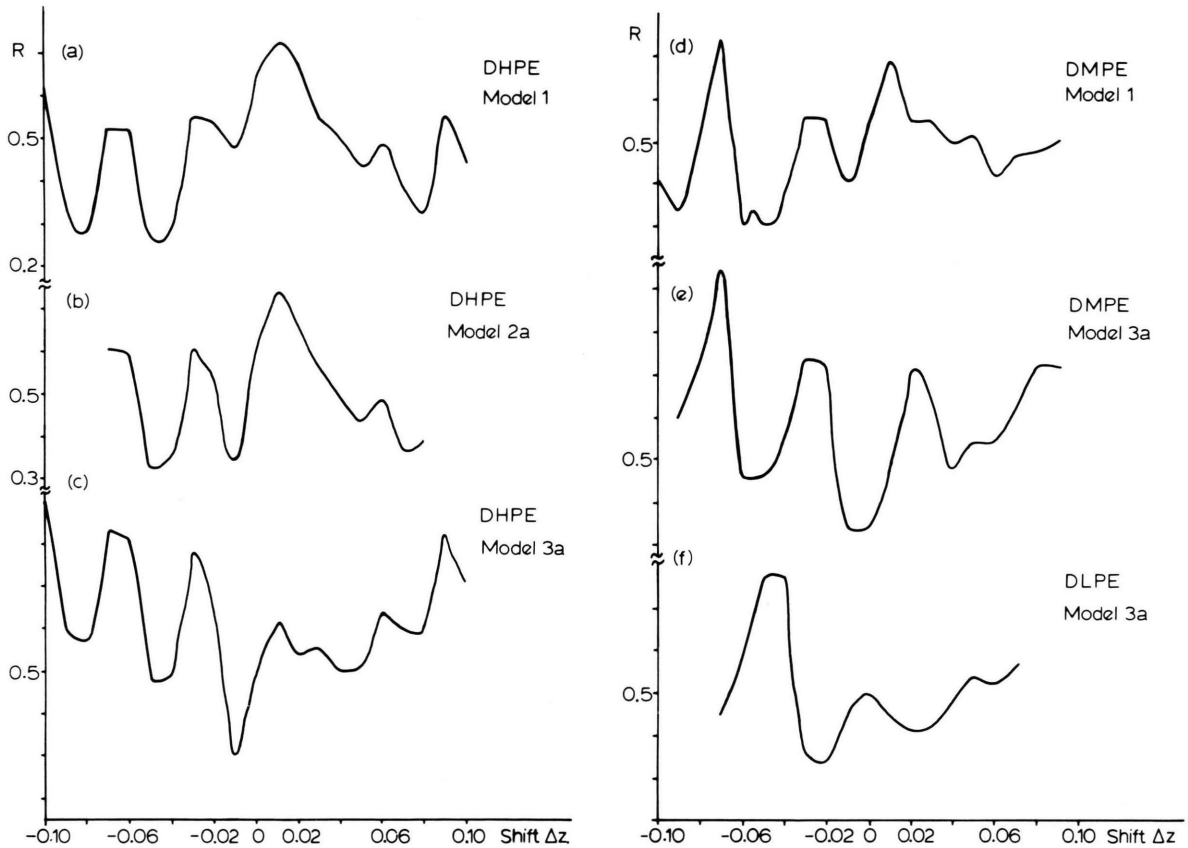

Fig. 6. Rigid body translational searches using electron diffraction data (a) DHPE, low temperature factors, no correction for lamellar curvature, (b) DHPE, high temperature factors, no correction for lamellar curvature, (c) DHPE low temperature factors, correction for lamellar curvature, (d) DMPE, low temperature factors, no correction for lamellar curvature (e) DMPE, low temperature factors, correction for lamellar curvature, (f) DLPE, low temperature factors, correction for lamellar curvature.

with corrected intensity from dihexadecyl phosphatditylethanolamine, a minimum is found again corresponding to a phosporus position at $z \cdot c =$ 0.43 Å. In the more extreme case, i.e. if only a central section of the intensity of each reflection is measured by the densitometer, then the correction is similar to (3) above and the rigid body search with corrected data gives a minimum again at $z \cdot c = 2.23$ Å for phosphorus. A comparison of calculated and observed structure factors is shown in Table 3 which represents a correction to observed data according to (3).

Electrostatic Potential Maps

Electrostatic potential maps are calculated in one dimension using the phases obtained from the *R*-value minimum which best conforms to the known crystal structure (see Table 2) and observed structure factors respectively assuming a perfect and a distorted crystal (Figure 7). These are compared to maps made from calculated structure factors based on the three models discussed above. Since the features of a structure map largely depend on the phase assignments [34], it is not surprising that these are all very similar to one another. However, a comparison of corresponding densities for a map obtained from calculated structure factor to maps calculated with observed data respectively assuming a perfect or a distorted crystal (Fig. 8) readily shows that the least overall deviation from the line of perfect correlation occurs when a correction is made for crystal distortion. On a quantitative basis, using a curve fitting routine and assuming a linear relationship between the two data sets, it is found

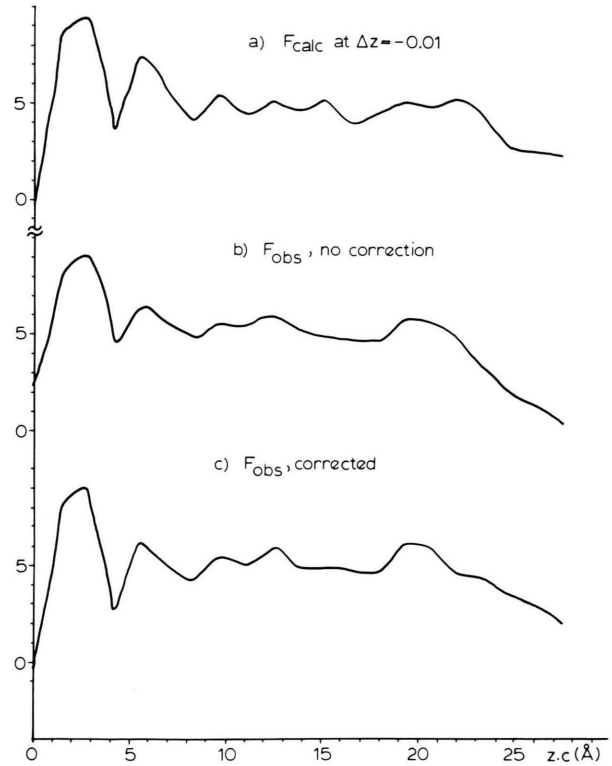

Fig. 7. Electrostatic potential maps for 1,2-dihexadecyl-*sn*-glycerophosphoethanolamine (DHPE) using: (a) F_c with phases at shift $\Delta z = -0.01$, (b) F_{obs} with same phases but no correction for lamellar curvature and (c) F_{obs} with same phases but also with correction for lamellar curvature. The first and largest peak on the left corresponds to the phosphoethanolamine moiety, the second to the glycerol region and the latter region to the long chains (compare to Figure 3).

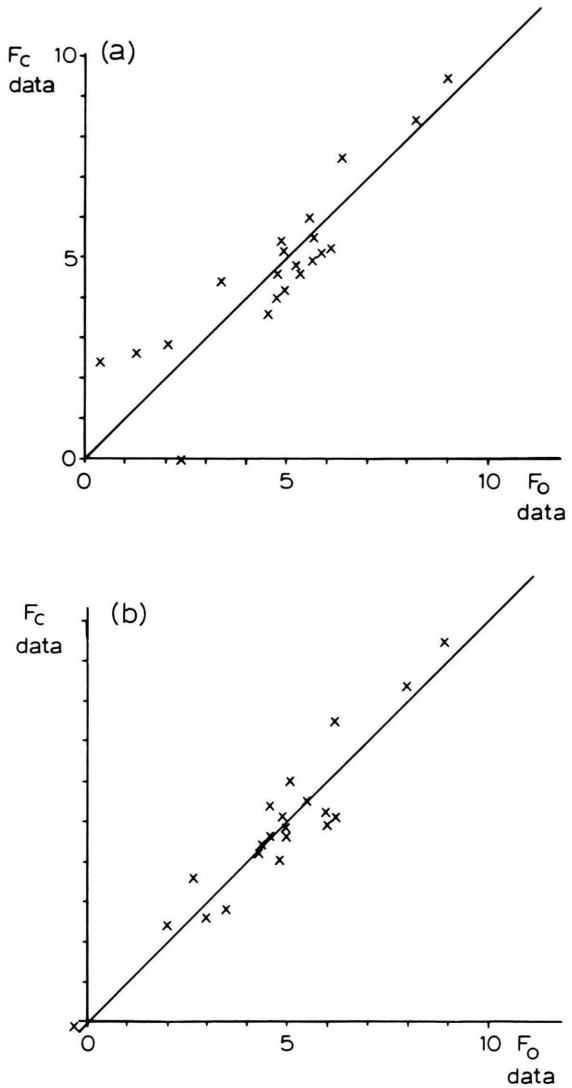

Fig. 8. Correlation of density in electrostatic potential maps in Fig. 7. (a) Comparison of map density of Fig. 7a with Figure 7b; (b) comparison of map density of Fig. 7a with Figure 7c. The line at 45° indicates a perfect correlation with no need for a scaling factor (only approximately true, see text). The second comparison of structures is found to give best agreement.

that a scale factor should be applied in both comparisons. After this, the respective correlation coefficients [35] for the maps calculated from uncorrected observed structure factors to the one obtained from calculated structure factors are 0.88 and 0.94.

Discussion

Refinement space is multivariate and with a number p parameters being refined against n observed data, there can be many local minima in the crystallographic residual which may be nearly the same value. The possibility to distinguish a correct solution among alternative structural models can be particularly difficult when there are a small number of observed data [27]. In the rigid body translational search of the dimyristoyl phosphatidylethanolamine (DMPE) crystal structure using x-ray data discussed above, the conformational integrity of a shorter chain homolog is assumed to be a reasonable model. Nevertheless there are at least three variables in this analysis, i.e. scale factor, translation coordinate and overall temperature

factor for $n = 15$ observed data. Following the statistical analysis given by Hamilton [36] (and assuming unit weight for calculation for the residual), the significance of an R-factor is based on

$$\mathscr{R}_{p,\,n-p,\,\alpha} = \left[\frac{p}{n-p} F_{p,\,n-p,\,\alpha} + 1 \right]^{1/2},$$

where F is a distribution function and α is the significance level of the test. Thus for two structural models with R-values R_1 and R_0 where R_0 is the smallest, the model with R_1 can be rejected only if $R_1 > \mathscr{R}_{p,\,n-p,\,\alpha} R_0$. In the x-ray study then, $p = 3$, $n - p = 12$ and from Table 4 of Hamilton's book [36] $F_{3,\,12,\,0.05} = 3.4903$ leading to $\mathscr{R}_{3,\,12,\,0.05} = 1.37$. Thus, although the lowest R-value minimum found for DMPE is 0.16, within these refined parameters any other model up to $R = 0.22$ cannot be excluded. From the sharpness of minima in Fig. 4, other minima in the residual curve for which only molecular translation is changed can be clearly rejected. The structural result also appears to be meaningful and, as mentioned above, is consistent with a one dimensional neutron diffraction structure analysis on a chiral dipalmitoyl homolog [10].

The picture is not so straightforward for the structure determination with electron diffraction data. In our considerations above we can include at least five variable parameters – i.e. scale factor, two temperature factors (for polar region and chains), molecular shift and crystal texture (the latter variable is assumed in the x-ray refinement). For the phospholipid DHPE which give the "best" structural results (i.e. lowest R-factor), $p = 5$ and $n = 16$. Testing at the $\alpha = 0.05$ confidence level, we find

$$\mathscr{R}_{5,\,11,\,0.05} = \left[\frac{5}{11} \cdot 3.2039 + 1 \right]^{1/2} = 1.57.$$

Hence, although the lowest R-value shown in Table 2 is 0.24, we can accept models with residuals up to 0.38 as being equally probable. This includes a model where the data are corrected for lattice distortion and which refines to a position similar to the one found in the x-ray analysis. Compared to earlier structure analyses with x-ray data [30], the R-value for the correct solution is not unreasonable.

The correctness of these assumptions can be supported with other data. To review, comparison of unit cell "long spacings" from these chiral phosphatidylethanolamines to those from the racemic forms shows that they are very similar and are likely not to be a tilted polymorph (Table 1). Electron diffraction data from solution grown crystals, which only allow one to discern the features of the acyl chain packing [37], also indicate the chain axes to be untilted and to pack in a methylene subcell similar to the one found for the racemic DLPE [19, 22]. Chains of the dialkyl lipid DHPE has been shown to pack in the hexagonal methylene subcell [19] which is also untilted. Electron micrographs in Fig. 2 clearly indicate that the crystals undergo a plastic deformation of the lamellae which has already been shown for solution grown samples to be a property peculiar to such lipids [38]. This justifies the type of correction used to the observed diffraction data and leads to the identification to a physically resonable packing model similar to the results obtained from x-ray data and single crystal determinations. Recalculation of Patterson maps after the observed data are corrected for crystal texture, still gives a pronounced peak near 4.0 Å but also improves the visibility of peaks due to longer vector interactions. Calculations of Patterson maps at various translational positions of the phasing model was shown to provide the best match to the map produced from observed data (i.e. a cross-correlation) when the physically reasonable solution is reached. Such a match of autocorrelation functions may therefore be more meaningful than R-factor minima.

It is also important to stress here that electron diffraction structure analyses cannot be carried out in a dogmatic way – i.e. a universal model for crystal texture cannot be applied in all cases [39]. For example, the best description of many solution-grown samples, i.e. a bend deformed perfect crystal, also appears to hold for the best epitaxially-crystallized polymethylene crystals such as n-paraffins for quantitative structure analysis [40]. With the recent demonstration of lattice imaging for both solution- [41] and epitaxially- [25] crystallized paraffin crystals, it is nevertheless important to obtain even low resolution (e.g. 16 Å) images of the crystal texture first in order to discern what model is best applied to a particular electron crystal structure analysis. Only then, as demonstrated here, can structural interpretations be made which have physical meaning.

[1] C. R. Worthington and T. J. McIntosh, Nature New Biology **245,** 97 (1973).
[2] D. L. D. Caspar and D. A. Kirschner, Nature New Biology **231,** 46 (1971).
[3] D. Harker, Biophys. J. **12,** 1285 (1972).
[4] G. I. King, Acta Crystallogr. **A 31,** 130 (1975).
[5] Y. K. Levine, Progr. Surf. Science **3,** 279 (1973).
[6] N. P. Franks, J. Mol. Biol. **100,** 345 (1976).
[7] D. L. Worcester and N. P. Franks, J. Mol. Biol. **100,** 359 (1976).
[8] G. Büldt, U. Gally, J. Seelig, and G. Zaccai, J. Mol. Biol. **134,** 673 (1979).
[9] G. Zaccai, G. Büldt, A. Seelig, and J. Seelig, J. Mol. Biol. **134,** 693 (1979).
[10] G. Büldt and J. Seelig, Biochemistry **19,** 6170 (1980).
[11] P. B. Hitchcock, R. Mason, K. M. Thomas, and G. Shipley, Proc. Nat. Acad. Sci. USA **71,** 3036 (1974).
[12] M. Elder, P. Hitchcock, R. Mason, and G. G. Shipley, Proc. Roy. Soc. London **A 354,** 157 (1977).
[13] R. H. Pearson and I. Pascher, Nature **281,** 499 (1979).
[14] K. Harlos, H. Eibl, I. Pascher, and S. Sundell, Chem. Phys. Lipids **34,** 115 (1984).
[15] I. Pascher and S. Sundell, Biochim. Biophys. Acta **855,** 68 (1986).
[16] P. B. Hitchcock, R. Mason, and G. G. Shipley, J. Mol. Biol. **94,** (1974).
[17] J. C. Wittmann and R. St. J. Manley, J. Polym. Sci.-Polym. Phys. Ed. **16,** 1891 (1978).
[18] D. L. Dorset, W. Pangborn, and A. J. Hancock, J. Biochem. Biophys. Methods **8,** 29 (1983).
[19] D. Chapman, P. Byrne, and G. G. Shipley, Proc. Roy. Soc. London **A 290,** 115 (1966).
[20] M. Suwalsky and E. Knight, Z. Naturforsch. **37c,** 1157 (1982).
[21] D. L. Dorset and W. A. Pangborn, Chem. Phys. Lipids **30,** 1 (1982).
[22] D. L. Dorset, Biochim. Biophys. Acta **424,** 396 (1976).
[23] H. Hauser, I. Pascher, R. H. Pearson, and S. Sundell, Biochim. Biophys. Acta **650,** 21 (1981).
[24] J. R. Fryer and D. L. Dorset, J. Microsc. (Oxford) (1986), in press.
[25] J. R. Fryer, Inst. Phys. Conf. Ser. **61,** 19 (1981).
[26] P. A. Doyle and P. S. Turner, Acta Crystallogr. **A 24,** 390 (1986).
[27] G. H. Stout and L. H. Jensen, X-Ray Structure Determination. Macmillan, New York 1968, pp. 309–314, p. 278.
[28] J. M. Cowley, Diffraction Physics, 2nd Edition, North-Holland, Amsterdam 1981, pp. 238–243.
[29] I. Pascher, S. Sundell, and H. Hauser, J. Mol. Biol. **153,** 807 (1981).
[30] R. S. Khare and C. R. Worthington, Biochim. Biophys. Acta **514,** 239 (1978).
[31] B. K. Vainshtein, Diffraction of X-rays by Chain Molecules, Elsevier, Amsterdam 1966, p. 386.
[32] R. J. Cella, B. Lee, and R. E. Hughes, Acta Crystallogr. **A 26,** 118 (1970).
[33] B. K. Vainshtein, Sov. Phys.-Crystallogr. **2,** 334 (1957).
[34] G. N. Ramachandran and R. Srinivasan, Fourier Methods in Crystallography, Wiley-Interscience, New York 1970, pp. 62–68.
[35] P. R. Bevington, Data Reduction and Error Analysis for the Physical Sciences, McGraw-Hill, New York 1969, pp. 119–133.
[36] W. C. Hamilton, Statistics in Physical Sciences, Ronald, New York 1964, pp. 157–162.
[37] D. L. Dorset, Ultramicroscopy **12,** 19 (1983).
[38] D. L. Dorset, S. W. Hui, and C. M. Strozewski, J. Supramol. Struct. **5,** 1 (1976).
[39] D. L. Dorset, J. Electron Microsc. Techniques **2,** 89 (1985).
[40] B. Moss, D. L. Dorset, J. C. Wittmann, and B. Lotz, J. Polym. Sci.-Polym. Phys. Ed. **22,** 1919 (1984).
[41] F. Zemlin, E. Reuber, E. Beckmann, E. Zeitler, and D. L. Dorset, Science **229,** 461 (1985).
[42] T. H. Bevan and T. Malkin, J. Chem. Soc. **1951,** 2267.